High-temperature spin dynamics in CMR manganites: ESR and magnetization

M. T. Causa, M. Tovar, A. Caneiro, F. Prado, G. Ibañez, C. A. Ramos, A. Butera, and B. Alascio
Centro Atómico Bariloche and Instituto Balseiro, Comisión Nacional de Energía Atómica and Universidad Nacional de Cuyo, 8400 San Carlos de Bariloche, Río Negro, Argentina

X. Obradors and S. Piñol
Instituto de Ciencia de Materiales de Barcelona, 08193 Bellaterra, Spain

F. Rivadulla, C. Vázquez-Vázquez, M. A. López-Quintela, and J. Rivas
Universidad de Santiago de Compostela, 15700 Santiago de Compostela, Spain

Y. Tokura
Department of Physics, University of Tokyo, Tokyo, 113, Japan

S. B. Oseroff
San Diego State University, San Diego, California 92182
(Received 5 December 1997)

We have performed electron spin resonance (ESR) and dc susceptibility measurements in Mn perovskites up to 1000 K. Assuming an effective Heisenberg-like interaction for $Mn^{3+}-Mn^{4+}$ spin pairs, the dc susceptibility, $\chi_{dc}(T)$, is well described in the paramagnetic regime by the constant coupling approximation. Absolute determination of the ESR intensity indicates that all Mn spins contribute to the ESR line in the temperature range studied. The ESR linewidth can be described by $\Delta H_{pp}(T)=\Delta H_{pp}(\infty)\ [C/T\chi_{dc}(T)]$, thus presenting a universal behavior in a temperature scale normalized to T_c. A single relaxation mechanism, related to spin-only interactions, explains the T dependence of $\Delta H_{pp}(T)$ for all the compounds studied: $La_{0.67}Ca_{0.33}MnO_3$, $La_{0.67}Sr_{0.33}MnO_3$, $Pr_{0.67}Sr_{0.33}MnO_3$, and $La_{0.67}Pb_{0.33}MnO_3$. The dc susceptibility and the ESR linewidth and intensity all reflect the progressive importance of magnetic clustering below $\approx 2T_c$. [S0163-1829(98)08629-9]

I. INTRODUCTION

The discovery of colossal magnetoresistence (CMR) in manganese oxides has renewed the interest in these materials,[1] where a high correlation between structural, transport, and magnetic properties is found. Perovskites of general formula $A_{1-x}A'_xMnO_3$ ($A=La,Pr,\ldots$; $A'=Ca,Sr,Ba,\ldots$) with $x\simeq 0.3$ exhibit CMR effects in the vicinity of the paramagnetic (PM) to ferromagnetic (FM) transition temperature, T_c. These oxides show intense electron spin resonance (ESR) lines in the PM phase with large variations of the line parameters[2] as a function of T. A large increase in intensity near T_c, in coincidence with a divergent behavior of the static susceptibility, reflects the strong exchange coupling between the resonant species.[2–4] However, attempts to describe the measured ESR intensity, $I(T)$, with a simple Curie-Weiss (CW) law were not satisfactory in the full PM temperature range and it was suggested[2] that the formation of $Mn^{3+}-Mn^{4+}$ spin clusters, when T_c is approached from above, should be taken into account beyond the Weiss molecular-field approximation. The peak-to-peak linewidth $\Delta H_{pp}(T)$ shows a linear T dependence above T_c that was interpreted in terms of a single-phonon spin-lattice relaxation mechanism.[3,4] Close to the high-temperature limit of the reported data,[3,4] a tendency to saturation was observed. A crossover from a bottlenecked regime, where Mn^{3+} and Mn^{4+} ions are strongly coupled, to an isothermal one was proposed[4] as an explanation of this slope change in $\Delta H_{pp}(T)$. Systematic studies in an extended temperature range were required[3] in order to confirm these observations and correlate the results with theoretical models for CMR involving double exchange and electron-phonon interactions. For this reason, we have performed ESR and magnetization measurements in a series of perovskite compounds in an extended range of temperatures, up to 1000 K.

II. EXPERIMENTAL DETAILS

Ceramic samples of $La_{0.67}Ca_{0.33}MnO_3$ were prepared by the nitrate method using La_2O_3 (99.999%), CaO (99.9995%), and metallic Mn (99.99%). The oxides were preheated at 1200 °C under vacuum in order to eliminate adsorbed or chemically bound CO_2 and water vapor. Stoichiometric amounts were subsequently weighed in a dry box and dissolved in nitric acid. The compound was synthesized at 1250 °C, with a final sintering process at 1450 °C. $La_{0.67}Sr_{0.33}MnO_3$ and $Pr_{0.67}Sr_{0.33}MnO_3$ powder samples were prepared by solid-state reactions of Pr_6O_{11}, La_2O_3, $SrCO_3$, and a mixture of MnO_2 and MnO, all of them at least 99.995% pure. After intermediate heat treatment at 1100 and 1200 °C, pressed pellets were kept at 1300 °C for 100 h. We have also measured single crystals of $La_{0.67}Sr_{0.33}MnO_3$ and $La_{0.67}Pb_{0.33}MnO_3$ that were prepared as described in Refs. 1 and 5.

Structure and phase purity were controlled by powder x-ray diffraction. The powder pattern for $La_{0.67}Ca_{0.33}MnO_3$ and

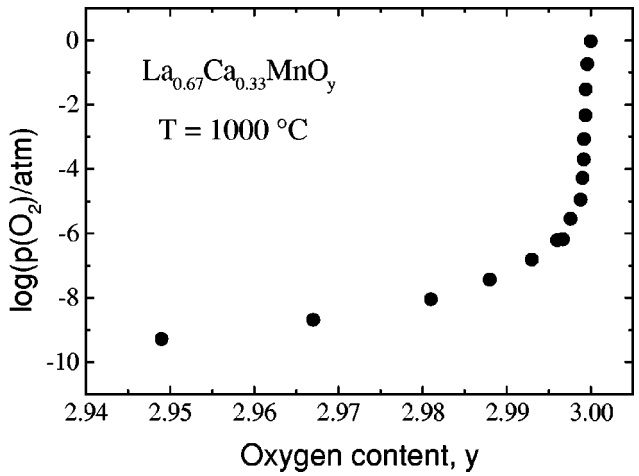

FIG. 1. log[$p(O_2)$/atm.] vs oxygen content ''y'' at 1000 °C for $La_{0.67}Ca_{0.33}MnO_y$.

$Pr_{0.67}Sr_{0.33}MnO_3$ were indexed on the basis of the $Pbnm$ space group. Rietveld refinement gave $a=5.4766$ Å, $b=5.4609$ Å, and $c=7.7153$ Å for $La_{0.67}Ca_{0.33}MnO_3$ and $a=5.4570$ Å, $b=5.4896$ Å, and $c=7.7044$ Å for $Pr_{0.67}Sr_{0.33}MnO_3$. The pattern of $La_{0.67}Sr_{0.33}MnO_3$ corresponds to a rhombohedral structure $R\bar{3}c$ with $a=5.5013$ Å and $c=13.3600$ Å. The composition homogeneity of a sample of $La_{0.67}Ca_{0.33}MnO_3$ was checked by scanning electron microscopy and electron-diffraction spectroscopy analysis and found better than 1.5%. The oxygen stoichiometry was measured at 1000 °C for a sample of $La_{0.67}Ca_{0.33}MnO_y$ by thermogravimetry[6] as a function of the $p(O_2)$ in $Ar-O_2$ and $CO-CO_2$ atmospheres. The shape of the isotherm shown in Fig. 1 assures that the oxygen content $y=3.000(2)$ is obtained for $10^{-4}\leqslant p(O_2)\leqslant 1$ atm. Thus, our samples were quenched after annealing at 1000 °C in air.

The dc magnetic susceptibility $\chi_{dc}(T)$ was measured from 250 to 1200 K, using a Faraday balance magnetometer. ESR measurements were performed at 1.2 GHz (L band), 9.4 GHz (X band) and 34 GHz (Q band) with an ESP-300 Bruker spectrometer from 200 to 350 K. For the X band, the measurements were extended up to 1000 K using a 4114HT Bruker cavity.

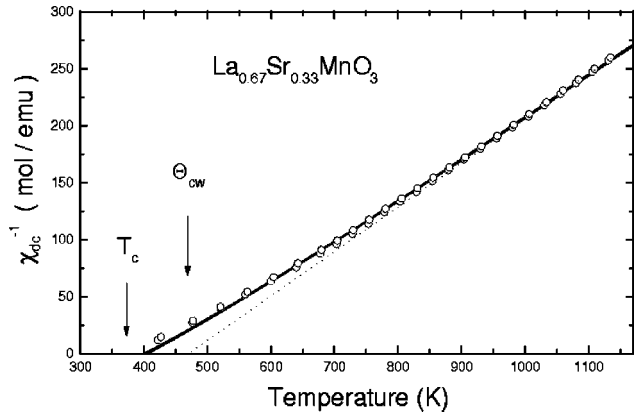

FIG. 2. dc susceptibility for $La_{0.67}Sr_{0.33}MnO_3$. Circles, experimental data. Solid and dotted lines are fits to the constant-coupling and Curie-Weiss models, respectively.

TABLE I. Values for the Curie constant, Curie-Weiss and critical temperatures, and exchange constant obtained from susceptibility measurements.

Compound	C (emu K/mol)	Θ (K)	T_c (K)	T_c/Θ	J/k_B
$La_{0.67}Ca_{0.33}MnO_3$	2.8(1)	368	260	0.69	49
$La_{0.67}Sr_{0.33}MnO_3$	2.6(1)	470	376	0.80	62
$Pr_{0.67}Sr_{0.33}MnO_3$[a]	2.6(1)	350	295	0.84	46
$La_{0.67}Pb_{0.33}MnO_3$			342		

[a]Values determined after subtraction of the Pr^{3+} contribution to the measured susceptibility.

III. EXPERIMENTAL RESULTS

At high temperatures, $\chi_{dc}(T)$ follows in all cases a FM Curie-Weiss temperature dependence, $\chi_{dc}(T)=C/(T-\Theta)$. For temperatures below 1.5 Θ the curve for the inverse susceptibility vs T shows a positive curvature (see Fig. 2) and $\chi_{dc}(T)$ tends to diverge at $T_c<\Theta$. From the linear behavior $\chi_{dc}^{-1}(T)$, for $T>2\Theta$, we have determined the Curie constant C and extrapolation to lower temperatures gives Θ. In Table I, we present the values obtained for C, T_c, and Θ.

In the PM temperature range the ESR spectrum consists of a single line with g values given in Table II, which are constant and independent of the microwave frequency at high temperatures. The line shape for sintered pellets and single crystals was Dysonian. Lorentzian lineshapes were obtained when the ceramic samples were reduced to fine powder, as discussed in Ref. 7. For Dysonian line shapes, linewidths and resonant fields were derived following the method proposed by Peter *et al.*[8]

A. ESR linewidth

When the ESR signals are intense, as it is usually the case for FM materials near T_c even for relatively small samples, the measured linewidth is strongly dependent on the number of spins in the sample. We have found that the ESR signal corresponding to $La_{0.67}Ca_{0.33}MnO_3$ powder samples of 10–15 mg presented a linewidth significantly larger than samples of 1 mg. Near room temperature, where $\chi_{dc}(T)$ is large and $\Delta H_{pp}(T)$ approaches its minimum value, this effect is most noticeable with a linewidth increase up to a factor of ≈ 2 (see Fig. 3). These sample size effects arise from overloading the cavity through magnetic losses.[9] If these losses are not large enough to drive the diode detector out of linearity, the ESR line remains Lorentzian, although with a larger linewidth. When the microwave frequency is fixed to the loaded cavity, it is given approximately by

TABLE II. ESR parameters.

Compound	g factor	$\Delta H_{pp}(\infty)$ [Gauss]
$La_{0.67}Ca_{0.33}MnO_3$	1.992(3)[a]	2400
$La_{0.67}Sr_{0.33}MnO_3$	1.99(1)	2700
$Pr_{0.67}Sr_{0.33}MnO_3$	2.00(1)	4500
$La_{0.67}Pb_{0.33}MnO_3$	1.98(1)	2600

[a]Value determined from Q-band data.

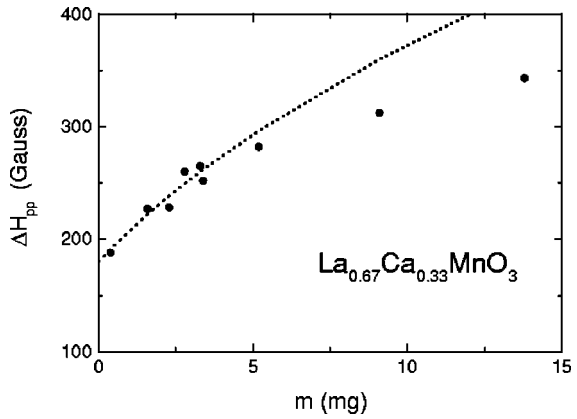

FIG. 3. Variations of the observed linewidth as a function of the sample mass (•). Dashed line is the correction factor $(1+b)^{1/2}$ as discussed in the text.

$$\Delta H_{pp}^{obs} = \Delta H_{pp}(1+\mathrm{b})^{1/2}, \tag{3.1}$$

with $b=(4\pi/3)\,\eta Q_L \chi_{esr}\omega/\gamma\Delta H_{pp}$, where χ_{esr} is the static susceptibility corresponding to the resonant species, η is the filling factor, and Q_L is the loaded Q of the microwave cavity.

As seen in Fig. 3, we found that although Eq. (3.1) qualitatively describes the observed variations for relatively small samples, quantitative corrections would not be appropriate for the largest samples. Thus, numerical corrections based on this equation may not be reliable. In order to avoid these difficulties, we have repeated the experiments at each temperature with different amounts of powder material and, when necessary, extrapolated the data to zero mass.

As a function of T, the ESR linewidth showed in all cases a behavior similar to that described in previous papers:[2] $\Delta H_{pp}(T)$ decreases with decreasing temperature. On approaching T_c from above, $\Delta H_{pp}(T)$ often goes through a minimum at $T_{min} > T_c$. The value of T_{min}, the measured linewidth at this temperature, and especially the rate of increase below it have been reported[10] as extremely sample dependent. It has been subsequently suggested[11] that this behavior may be associated with some magnetic inhomogeneity of the samples arising from local variations of chemical composition or oxygen stoichiometry. We are interested in the study of the relaxation mechanisms in the PM regime and it is then very important to ensure that the measured T dependence are not spurious effects related to the quality of the samples.

We have measured samples of different origin prepared either as ceramic materials or single crystals. A powder ceramic sample of $La_{0.67}Ca_{0.33}MnO_3$ was studied in detail around T_c and Fig. 4 shows the passage from the PM to the FM regime. For $T=272$ K, a single line, 300 Gauss wide with no structure, was observed. Below this temperature a new line separates from the principal and shifts to lower field. The intensity is progressively transferred from one to the other and below 269 K a single line is again obtained. The field spread of the spectrum at a given temperature can be interpreted[10–12] in terms of a T_c distribution. The narrowness of this distribution (less than 3 K) that could be associated with the behavior in Fig. 4 indicates the good quality of the sample.

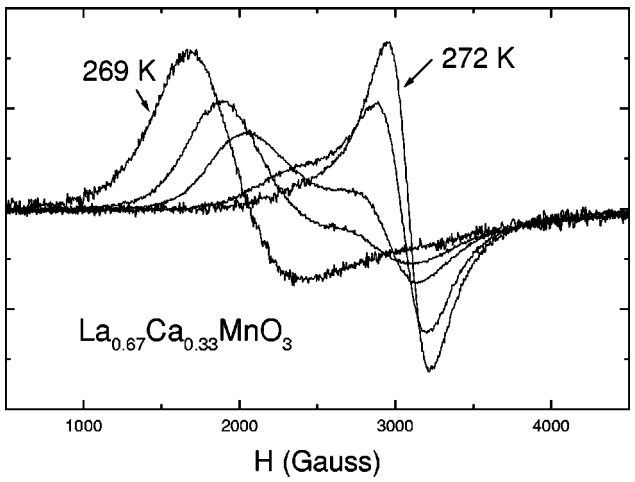

FIG. 4. X-band ESR spectra of powder ceramic $La_{0.67}Ca_{0.33}MnO_3$ for different temperatures in the vicinity of T_c.

We present in Fig. 5 some of the results obtained for $La_{0.67}Sr_{0.33}MnO_3$. For powder ceramic samples (open squares and triangles) a minimum linewidth of 130 Gauss was measured at $T_{min} \approx 1.04\,T_c$. Below this temperature the linewidth increases rapidly. On the other hand, the linewidth of a small flat single crystal ($1\times1\times0.1$ mm) remains approximately constant below T_c at about 70 G. The ESR spectrum for another single crystal, polished into a spherical shape of about 0.5 mm diameter, presents a distorted line shape with unresolved structure near and below T_c. The total peak-to-peak width (solid triangles in Fig. 5) reaches a minimum value of $\approx$150 G. The increase below T_{min} is similar to that observed for the case of powdered ceramic materials. The spread of the spectrum resembles the observation in Ref. 13 of a splitting of the ESR spectra for $La_{0.67}Pb_{0.33}MnO_3$ single crystals, due to the nonuniformity of the demagnetization tensor.

In addition to the sample-dependent effects, we have found strong dependence on the microwave frequency (or applied field at resonance) immediately above T_c, as shown in Fig. 6 for a sample of $La_{0.67}Ca_{0.33}MnO_3$. A similar variation with the microwave frequency was reported[13] for the splitting of the ESR spectrum on a $La_{0.67}Pb_{0.33}MnO_3$ single crystal. A comparison of both cases suggest that nonuniform

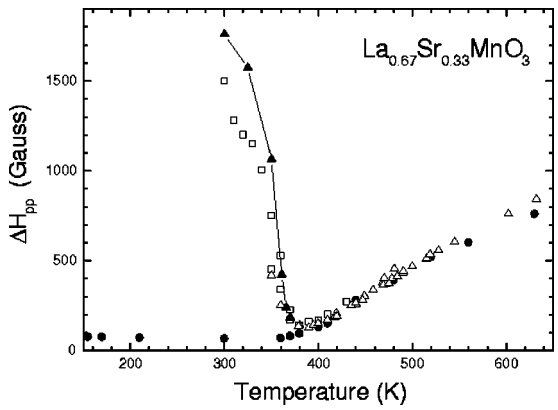

FIG. 5. $\Delta H_{pp}(T)$ vs T for $La_{0.67}Sr_{0.33}MnO_3$. Solid and open symbols corresponds to single crystals and powder ceramic samples, respectively.

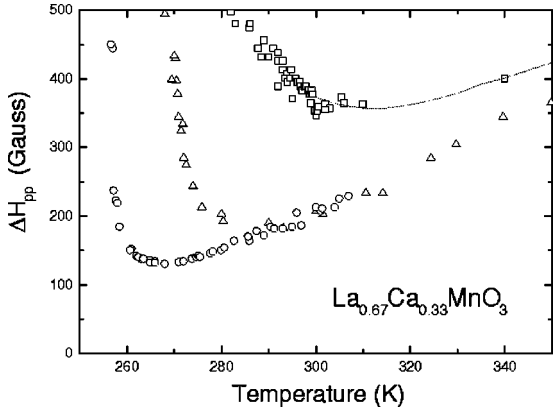

FIG. 6. $\Delta H_{pp}(T)$ vs T for the three microwave frequencies in the vicinity of T_{min}: (□) Q band, (△) X band, and (○) L band.

magnetization effects may originate this field dependence. Instead, the linewidths measured for different frequencies above T_{min} are coincident within a few percent.

Since the behavior observed between T_c and T_{min} is sample and field dependent and may confuse the analysis of the results in the paramagnetic regime, we have excluded this small temperature region from our analysis. Above T_{min}, instead, none of the effects described were found and the temperature dependence of the ESR linewidth in samples of different origin may be safely compared. In this temperature region $\Delta H_{pp}(T)$ was originally found to be almost linear with T, up to $\approx$600 K for $La_{0.67}Ca_{0.33}MnO_3$ (Ref. 2) and $La_{1-x}Sr_xMnO_3$ (Ref. 11). A small tendency to saturation was found[3,4] for $T\approx$600 K (close to the upper limit of the experiments) in the case of $La_{0.67}Ca_{0.33}MnO_3$ and $La_{0.8}Ca_{0.2}MnO_3$. We have extended the measurements up to 1000 K at the X band and found in all cases significant deviations from linearity at high temperatures. We show in Fig. 7 the results obtained for $\Delta H_{pp}(T)$ in $La_{0.67}Ca_{0.33}MnO_3$, $La_{0.67}Sr_{0.33}MnO_3$, $Pr_{0.67}Sr_{0.33}MnO_3$, and $La_{0.67}Pb_{0.33}MnO_3$. In all cases, full saturation was not achieved within our temperature limits.

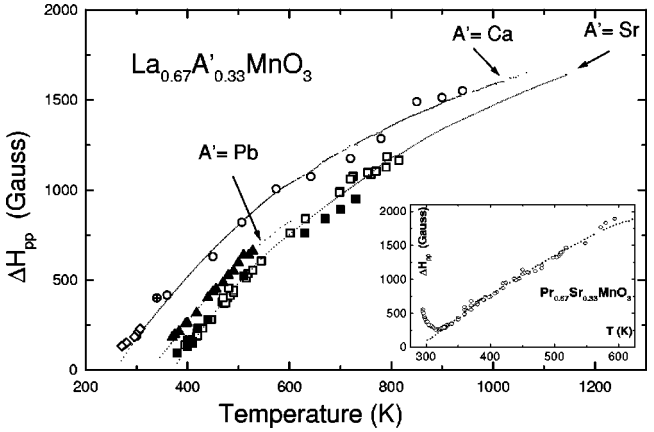

FIG. 7. X-band $\Delta H_{pp}(T)$ for $La_{0.67}A'_{0.33}MnO_3$, and $Pr_{0.67}Sr_{0.33}MnO_3$ (inset). Solid symbols correspond to single crystals. For $La_{0.67}Ca_{0.33}MnO_3$, L-band (◇) and Q-band (⊕) data are also shown. Dotted lines: Eq. (4.5) using the $\Delta H_{pp}(\infty)$ values of Table I and the measured χ_{dc} for each compound.

B. ESR intensity

The intensity of the ESR spectrum, $I(T)$, is an important parameter to identify the nature of the resonant entities[2–4,11] through the absolute value and temperature dependence of χ_{esr}. There are several experimental difficulties in the determination of $I(T)$ because the linewidth increases by a factor of 10 from T_{min} to the highest temperatures. In addition, the peak-to-peak amplitude of the measured derivative signal h_{pp} decreases three orders of magnitude in the same T range. This is a probable cause for the disagreement between recently reported results.[2–4,11] Based on these results, the authors have suggested that the observed signal is not the full ESR spectrum and would correspond to some of the magnetic species present in the sample. The remaining magnetic species would give rise to much broader ESR signals. Different possibilities have been proposed: Oseroff *et al.*[2] and Retori *et al.*[3] considered as the resonant entity a complex of $Mn^{3+}-Mn^{4+}$ spin clusters of increasing total average spin as T approaches T_c. In Ref. 4 the resonance was attributed to the Mn^{4+} ions, as part of a system of three components: Mn^{4+} ions, Mn^{3+} ions, and the lattice. On the other hand, Lofland *et al.*[11] found that all Mn ions contribute to the ESR signal, at least up to 600 K. In order to shed some light on this controversial subject, we have made a careful and detailed determination of $I(T)$ for $La_{0.67}Ca_{0.33}MnO_3$, up to 1000 K.

$I(T)$ was determined in two ways: (a) by numerical double integration of the measured spectra in a magnetic-field sweep of 10 $\Delta H_{pp}(T)$, and (b) approximating the area by the product $[\Delta H_{pp}(T)]^2 h_{pp}(T)$. Both methods gave results proportional to each other in the whole temperature range. Although the first method provides better accuracy for absolute values, the second one was preferred at high temperature because of the reduced signal-to-noise ratio of the ESR lines.

As in the case of $\Delta H_{pp}(T)$, the line intensity is modified by size effects due to magnetic losses and given approximately by[9]

$$I=\eta\chi_{esr}\omega Q_L(1+b)^{-1/2}. \tag{3.2}$$

When the condition $b\ll 1$ is not fulfilled, $I(T)$ is not linear in the sample mass. As already discussed for the case of linewidth determination, corrections based on Eq. (3.2) are of limited validity. We have avoided this problem by using small samples. In addition to the variations due to the sample size, $I(T)$ is modified by changes of Q_L as a function of temperature. These changes were partially caused by the experimental setup and we could not separate the possible contribution from dielectric losses in the sample arising from charge tranfer between M ions. Thus, in order to obtain $\chi_{esr}(T)$, we have renormalized the measured intensities using values of Q_L determined at each temperature. In Fig. 8, $\chi_{esr}(T)$ is shown and compared with $\chi_{dc}(T)$. We found that the temperature dependence is the same for both χ_{esr} and χ_{dc} in the whole PM temperature range.

Absolute values for $\chi_{esr}(T)$ were determined by comparison to a reference sample of the ''green phase'' Gd_2BaCuO_5, which follows a CW behavior[14] with $C=8.12$ emu K/mole Gd and $\Theta=-23$ K. We chose this sample because of the constant linewidth[14] as a function of T ($\approx$1100 G), which is

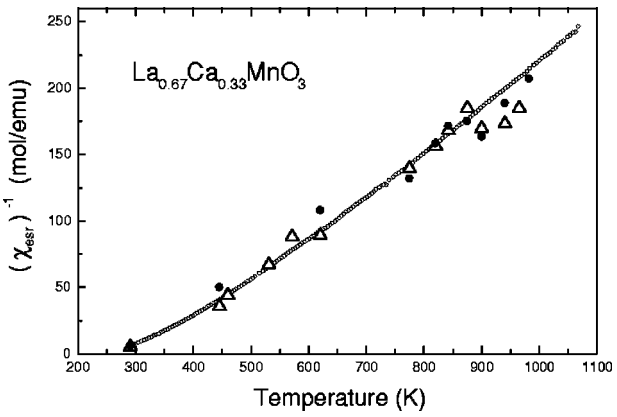

FIG. 8. $La_{0.67}Ca_{0.33}MnO_3$ ESR susceptibility vs T: (•) χ_{esr} obtained by numerical integration, (Δ) $\chi_{esr} \propto (\Delta H_{pp})^2 h_{pp}$. Small open circles, $(\chi_{dc})^{-1}$ vs T.

of the same order of magnitude as that of our samples. A careful determination was made for $La_{0.67}Ca_{0.33}MnO_3$ at two different temperatures and we obtained $\chi_{esr}(450\ \mathrm{K}) = 0.023(5)$ emu/mole and $\chi_{esr}(530\ \mathrm{K}) = 0.012(3)$ emu/mole. These values are in excellent agreement with the values measured for the dc susceptibility: $\chi_{dc}(450\ \mathrm{K}) = 0.024(3)$ emu/mole and $\chi_{dc}(530\ \mathrm{K}) = 0.015(2)$.

IV. DISCUSSION

The FM interaction between Mn ions present in CMR perovskites is commonly ascribed to the double exchange interaction proposed by Zener.[15] A simplified model for this interaction[16,17] indicates that the hopping of electrons between Mn ions connects them, forming high spin magnetic clusters that include the itinerant electron. The effective FM coupling of the Mn ions resulting from this model gives rise to a magnetic susceptibility[17] that may be described by an isotropic Heisenberg-like interaction between $Mn^{3+} - Mn^{4+}$ pairs.

$$\mathcal{H} = -2J \sum_{\langle i,j \rangle} S_1^i \cdot S_2^j + g\mu_B \sum_{i,j} (S_1^i + S_2^j) \cdot \mathbf{H}, \qquad (4.1)$$

where S_1 and S_2 identify the spin of Mn^{4+} and Mn^{3+} species, respectively, with $S_1 = \frac{3}{2}$ and $S_2 = 2$; $\mathbf{H}$ is the external magnetic field, and $\langle i,j \rangle$ runs over all possible $Mn^{3+} - Mn^{4+}$ pairs.

In the Weiss mean-field approximation (WMFA), Néel has shown[18] that in the case of a system of two different magnetic species, the $\chi_{dc}^{-1}(T)$ curve vs T is a hyperbola that, at high temperatures, presents a CW asymptotic behavior with

$$C = N_A g^2 \mu_B^2 [x S_1(S_1+1) + (1-x) S_2(S_2+1)]/3k_B, \qquad (4.2)$$

where x is the relative concentration of Mn^{4+} ions. For $x = 0.33$, the calculated value is $C = 2.64$ emu K/mol, which is close to the experimental results listed in Table I.

In the same limit, a CW temperature may be defined by the expression

$$k_B \Theta / J = (4z/3) x(1-x) S_1(S_1+1) S_2(S_2+1) / [x S_1(S_1+1) + (1-x) S_2(S_2+1)], \qquad (4.3)$$

where z is the number of nearest Mn neighbors. To obtain Eq. (4.3), we have assumed a random site occupation and, in this case, the average number of Mn^{4+} (Mn^{3+}) ions surrounding a Mn^{3+} (Mn^{4+}) is equal to z times their relative concentration. Using the measured values of Θ in Eq. (4.3), we have derived the values for J given in Table I.

The main assumption of the WMFA model is the statistical independence of the spins that neglect short-range order. Improvements on this model require a detailed treatment of the formation of magnetic clusters.[18] The constant-coupling approximation (CCA) takes into account the correlation between neighboring spins. We considered the magnetic system as an ensemble of spin pairs with an effective Hamiltonian

$$\mathcal{H} = -2J \mathbf{S}_1 \cdot \mathbf{S}_2 + g\mu_B (\mathbf{S}_1 + \mathbf{S}_2) \cdot [\mathbf{H} + \mathbf{H}_e], \qquad (4.4)$$

where $\mathbf{H}_e$ is an effective field (acting on the pair) determined by internal consistency requirements. For $T \to \infty$, both approximations predict the same result. However, as T approaches the ordering temperature, short-range order appears in the CCA and the ''effective field per neighbor'' increases less and less rapidly as compared to the WMFA. As a consequence, long-range order is achieved at a temperature $T_c < \Theta$, and the calculated susceptibility presents the positive curvature found experimentally for $\chi_{dc}^{-1}(T)$, as seen in Fig. 2.

The T dependence calculated in the CCA for $S = 3/2$ and $S = 2$ differ by less than 2%, when normalized to T_c. Thus, their average was used to fit the experimental data for $La_{0.67}Sr_{0.33}MnO_3$. As observed in Fig. 2, the agreement is excellent and the measured values for the ratio T_c/Θ in all samples, shown in Table I, are close to the calculated value $T_c/\Theta = 0.78$. The progressive clustering of the Mn ions, mediated by the hopping of the electron introduced by doping is consequently described by the CCA.

The ESR experiment probes the dynamics of the magnetic system. The coincidence of $\chi_{esr}(T)$ with $\chi_{dc}(T)$ in the whole PM range studied clearly indicates that all the Mn ions contribute to the observed ESR spectra. Thus, the ESR linewidth should be related to the relaxation mechanism of the coupled magnetic system. An exchange mechanism with bottlenecked spin relaxation between Mn^{4+} and Mn^{3+} magnetic subsystems[19] was proposed in Ref. 4 to describe the T dependence of $\Delta H_{pp}(T)$. This model assigns the ESR line to Mn^{4+} ions and predicts a FM Curie-Weiss-like behavior for the integrated intensity arising from the FM coupling of the two subsystems. However, it failed to reproduce correctly the measured intensities in the whole temperature range. The deviations from the predicted behavior were attributed to a possible breakdown of the bottleneck regime at high temperatures. The crossover to a nonbottlenecked state was correlated with the tendency to saturation of $\Delta H_{pp}(T)$. Since we have determined that all Mn spins contribute to the observed ESR line, and not only the Mn^{4+} ions, we must include the contribution to the resonance of the Mn^{3+} subsystem. Huber[20] has studied the problem of the resonance of two strongly coupled magnetic species and, in this case, a single ESR line should be observed in coincidence with our experiments.

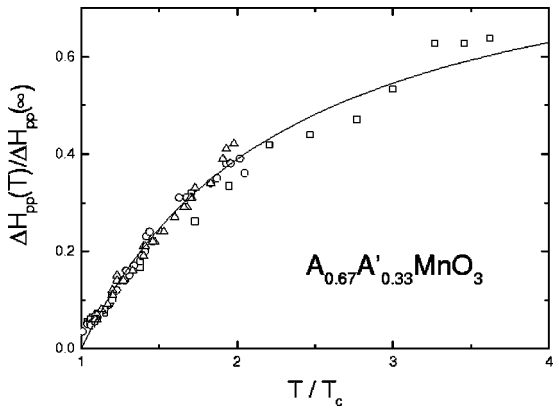

FIG. 9. $\Delta H_{pp}(T/T_c)/\Delta H_{pp}(\infty)$ vs T/Tc showing a universal behavior for the perovskites $A_{0.67}A'_{0.33}MnO_3$: (□) $A=$La, $A'=$Ca; (○) $A=$La, $A'=$Sr; (△) $A=$Pr, $A'=$Sr.

In treating the problem of the T dependence of ΔH_{pp} of magnetic compounds in the PM region, Dormann and Jaccarino[21] have argued, following Huber's[22] approach, that the main variation is given by the expression

$$\Delta H_{pp}(T) \propto [\chi_s(T)/\chi_{esr}(T)]\Delta H_{pp}(\infty), \qquad (4.5)$$

where $\chi_s(T)=C/T$ is the single-ion susceptibility and $\chi_{esr}(T)$ corresponds to the paramagnetic behavior of the coupled system. A similar result was obtained by Kotzler and Scheithe[23] from a phenomenological description in terms of modified Bloch equations. In order to use Eq. (4.5) for our system, the appropriate mixture of Mn^{3+} and Mn^{4+} single ions should be considered [see Eq. (4.2)] for $\chi_s(T)$. Accordingly, values for the total Mn static susceptibility $\chi_{dc}(T)$, measured on the same samples, were used to draw the continuous lines in Fig. 7. In the case of $Pr_{0.67}Sr_{0.33}MnO_3$, the Pr^{3+} contribution was previously subtracted. We found, in this way, an excellent agreement between the predictions of Eq. (4.5) and the experimental $\Delta H_{pp}(T)$ for all the CMR perovskites measured. This includes, not only the quasilinear behavior near T_c, but also the tendency to saturation at higher temperatures. A universal T dependence for the ESR linewidth in a T scale normalized to T_c ($t=T/T_c$) was found for $\Delta H_{pp}(t)/\Delta H_{pp}(\infty)$, as illustrated in Fig. 9, where a comparison is made with the function $C/[t\chi(t)]$, calculated in the CCA. The normalizing parameter $\Delta H_{pp}(\infty)$ is given in Table II. Thus, we conclude that the T dependence arises solely from the variation of $\chi(T)$ in the prefactor of Eq. (4.5). Therefore, we found no need for the inclusion of any extra T-dependent term in Eq. (4.5). This result makes doubtful previous interpretations[3] based on one-phonon spin-lattice relaxation mechanisms proposed by Huber and Seehra[24] for other insulating FM compounds. The universal behavior in a magnetic temperature scale also allows us to discard a possible influence of the high-T crystallographic transitions such as those reported[25] for $La_{0.7}(Ca_{1-p}Sr_p)_{0.3}MnO_3$, since the transition temperature decreases rapidly with p while T_c increases.

The limiting value $\Delta H_{pp}(\infty)$ in Eq. (4.5) corresponds to spin-only interactions, as discussed by Huber in Ref. 20. We found $\Delta H_{pp}(\infty) \cong 2600(200)$ G for the perovskites with $A=$La and $\Delta H_{pp}(\infty)=4500$ G in the case of $Pr_{0.67}Sr_{0.33}MnO_3$, where the nearest neighbors of the Mn ions are nonresonant magnetic species (Pr^{3+}). If the only anisotropic contribution were the dipole-dipole interaction, exchange-narrowed lines of only a few G would be expected,[20] using the J values of Table I. Therefore, other broadening mechanisms[26] must be considered in order to explain our results, probably associated with anisotropic exchange interactions.

V. CONCLUSIONS

We have measured in detail the temperature dependence of the dc susceptibility and the ESR line parameters in a wide temperature range for perovskite compounds $A_{1-x}A'_xMnO_3$ ($A=$La,Pr and $A'=$Ca,Sr,Pb) of different origin. The static magnetic susceptibility, $\chi_{dc}(T)$ is well described in the constant-coupling approximation, a mean-field model of the small cluster type. The integrated intensity of the ESR spectrum indicates that *all* Mn *spins* contribute to the resonance and not only the Mn^{+4} ions or some spin clusters. A divergent behavior for $\chi_{esr}(T)$ near T_c, in coincidence with $\chi_{dc}(T)$, reflects the importance of the FM coupling between Mn^{3+} and Mn^{4+} ions. The temperature dependence of the ESR linewidth may be described by a universal curve, whose temperature scale is associated with T_c. The behavior above T_c is determined solely by the temperature dependence of $\chi_{esr}(T)$. The infinite temperature linewidth is kept as an adjustable parameter that is related to spin-only interactions. We have found no evidence of a spin-phonon contribution to the experimental linewidth.

ACKNOWLEDGMENTS

We like to thank D. L. Huber for helpful comments and private communications. We acknowledge partial support of EEC (Commission DGXII, Contract No. GCI1C792-0087), CONICET-Argentina (LANAIS # 34 - Condensed Matter and PIP 4947), Project Ref: PB94-1528 DGICYT, Ministerio de Educación y Ciencia (Spain), and NSF-DMR-9705155 and 9400439.

[1] A. Urushibara, Y. Moritomo, T. Arima, A. Asamitsu, G. Kido, and Y. Tokura, Phys. Rev. B **51**, 14 103 (1995).

[2] S. B. Oseroff, M. Torikachvili, J. Singley, S. Ali, S-W. Cheong, and S. Schultz, Phys. Rev. B **53**, 6521 (1996).

[3] C. Rettori, D. Rao, J. Singley, D. Kidwell, S. B. Oseroff, M. T. Causa, J. J. Neumeier, K. J. McClellan, S-W. Cheong, and S. Schultz, Phys. Rev. B **55**, 3083 (1997).

[4] A. Shengelaya, Guo-meng Zhao, H. Keller, and K. A. Müller, Phys. Rev. Lett. **77**, 5296 (1996).

[5] F. Sandiumenge, S. Gali, and S. Piñol, Philos. Mag. Lett. **76**, 41 (1997).

[6] A. Caneiro, P. Bavdaz, J. Fouletier, and J. P. Abriata, Rev. Sci. Instrum. **53**, 1072 (1982).

[7] M. S. Seehra, M. M. Ibrahim, V. S. Babu, and G. Srinivasan, J. Phys.: Condens. Matter **8**, 11 283 (1996).

[8] M. Peter, D. Shaltiel, J. H. Wenick, H. J. Williams, J. B. Mock,

and R. Sherwood, Phys. Rev. **126**, 1395 (1962).
[9] M. S. Seehra, Rev. Sci. Instrum. **39**, 1044 (1968).
[10] M. Domínguez, S.E. Lofland, S. M. Baghat, A. K. Raychaudhuri, H. L. Ju, T. Venkatesan, and R. L. Greene, Solid State Commun. **97**, 193 (1996).
[11] S. E. Lofland, P. Kim, P. Dahiroc, S. M. Bhagat, S. D. Tyagi, S. G. Karabashev, D. A. Shulyatev, A. A. Arsenov, and Y. Mukovskii, Phys. Lett. A **233**, 476 (1997).
[12] E. Granado, P. G. Pagliuso, J. A. Sanjurjo, C. Rettori, S. B. Oseroff, M. T. Causa, A. Butera, A. Caneiro, M. Tovar, J. J. Neumeier, K. J. McClellan, S-W. Cheong, R. Sánchez, J. Rivas, and S. Schultz, in *Noncrystalline and Nanoscale Materials*, edited by J. Rivas and M. A. Lopez-Quintela (World Scientific, Singapore, 1998), p. 105–115.
[13] C. A. Ramos, M. T. Causa, M. Tovar, X. Obradors, and S. Piñol, J. Magn. Magn. Mater. **177-181**, 867 (1998).
[14] G. F. Goya, R. C. Mercader, L. B. Steren, R. D. Sánchez, M. T. Causa, and M. Tovar, J. Phys.: Condens. Matter **8**, 4519 (1996).
[15] C. Zener, Phys. Rev. **82**, 403 (1951).
[16] J. Briático, B. Alascio, R. Allub, A. Butera, A. Caneiro, M. T. Causa, and M. Tovar, Phys. Rev. B **53**, 14 020 (1996).
[17] R. Allub and B. Alascio, Phys. Rev. B **55**, 14 113 (1997); (private communication).
[18] J. S. Smart, *Effective Field Theories of Magnetism* (Saunders, Philadelphia, 1966).
[19] J. E. Gulley and V. Jaccarino, Phys. Rev. B **6**, 58 (1972).
[20] D. L. Huber, Phys. Rev. B **12**, 31 (1975).
[21] E. Dormann and V. Jaccarino, Phys. Lett. **48A**, 81 (1974).
[22] D. L. Huber, J. Phys. Chem. Solids **32**, 2145 (1971).
[23] J. Kotzler and W. Scheithe, Phys. Status Solidi B **69**, 389 (1975).
[24] D. L. Huber and M. Seehra, J. Phys. Chem. Solids **36**, 723 (1975).
[25] P. G. Radaelli, M. Marezio, H. Y. Hwang, S-W. Cheong, and B. Batlogg, Phys. Rev. B **54**, 8992 (1996).
[26] B. R. Cooper and F. Keffer, Phys. Rev. **125**, 896 (1962); M. T. Causa and M. C. G. Passeggi, Phys. Lett. **98A**, 291 (1983).